Oil & Gas Science and Technology – Rev. IFP Energies nouvelles **75**, 53 (2020)

https://doi.org/10.2516/ogst/2020049

Available online at:
ogst.ifpenergiesnouvelles.fr

REGULAR ARTICLE OPEN ACCESS

Analysis of the impacts of relative permeability and mobility ratio on heterogeneity loss error during upscaling of geological models

Ameneh Darban, Mojtaba Ghaedi*, and Jafar Qajar

Department of Petroleum Engineering, School of Chemical and Petroleum Engineering, Shiraz University, 71946-84471 Shiraz, Iran

Received: 29 April 2020 / Accepted: 17 June 2020

Abstract. The detailed geological fine grids are upscaled to create reliably sized simulation coarse models to solve flow equations in a more efficient way. Any upscaling process results in a loss of accuracy, along with an increase of errors. Numerical dispersion, heterogeneity loss, and connectivity misrepresentation are responsible for the upscaling errors. Recognizing the source of each error, and the behavior of influential factors through upscaling process could provide an optimum level of upscaling and an evaluation of upscaling methods' accuracy. Despite the importance of upscaling error, little attention has been paid to this subject. This paper represents a rigorous analysis of the heterogeneity loss behavior associated with the relative permeability contrast and the mobility ratio under a waterflooding process. For this purpose, heterogeneous fine grid models are constructed by the fractional Brownian motion process. The models are upscaled by three upscaling factors. The models achieved are implemented to eliminate the impact of numerical error among upscaling errors in order to focus strictly on heterogeneity loss. Water–oil displacement simulation is then performed on fine and corresponding refined upscaled models at three different ratios of relative permeabilities and mobility ratios. In the next stage, the relation between flow performance error and heterogeneity loss is investigated by the heterogeneity loss plot. The slope of this plot provides the reservoir engineer an insight to evaluate the performance of upscaling methods and the behavior of the influential factors on upscaling errors. Moreover, by using the heterogeneity loss plot for each ratio, a limit of coarsening is presented. Based on the results, the heterogeneity loss error is affected more by the mobility ratio contrast than the relative permeability difference. Also, it is demonstrated that water-wet reservoirs with light oil are more sensitive to the level of upscaling.

1 Introduction

The drive for simulation processes originates from the importance of the remaining oil in place, and the need for accurate predictions of the oil and gas reservoirs' performance under different production scenarios and to lower the uncertainties and risks of failure of the costly operations (Stedinger *et al.*, 1984). Simulation can predict the displacement of the oil, gas and any fluids in reservoirs and consequently, it gives the reservoir engineer an insight to select the best scenarios for secondary and tertiary (Enhanced Oil Recovery [EOR]) production based on the reservoir conditions, fluids, facilities, etc. aiming to produce the most economically efficient production (Chen, 2007; Ertekin *et al.*, 2001). To simulate, one must first have a suitable model. The model used in simulation processes must reflect the behavior and properties of the actual reservoir. In the core samples, the properties are measured in centimeters (Pickup *et al.*, 1995). Therefore, the geological models typically contain 10^7–10^8 grid blocks or more, which are too wide for carrying out flow simulations using conventional techniques (Durlofsky, 2003; Thiele *et al.*, 1996). Engineering analysis needs to predict flow behavior repeatedly under different scenarios and operations. There is a little tendency to perform calculations on detailed geological models, because simulation on these models with significant numbers of grid blocks, in addition to requiring high hardware capabilities, they are also very time consuming (Christie, 1996). The number of grid blocks must, therefore, be reduced by upscaling which converts the geological model to simulation one. The upscaling process reduces the accuracy as it saves time, so it must be done in such a way to balance between these two (Ganjeh-Ghazvini *et al.*, 2015a; Misaghian *et al.*, 2018).

So far, most of the studies in the field of upscaling have focused on the analysis and developing upscaling methods (Aarnes *et al.*, 2005; Audigane and Blunt, 2004; Barker and Thibeau, 1997; Chen and Durlofsky, 2006; Christie *et al.*, 2007; Darman *et al.*, 2002; Durlofsky, 2005; Holden and Nielsen, 2000; Karimi-Fard and Durlofsky, 2016; Kyte

* Corresponding author: m.ghaedi@shirazu.ac.ir

and Berry, 1975; Liao *et al.*, 2019; Matthai and Nick, 2009; Peaceman, 1997; Zhang *et al.*, 2005). In these studies efforts were made to determine the equivalent permeability of a heterogeneous porous media (Renard and de Marsily, 1997; Sanchez-vila *et al.*, 2006). As an instance, Colecchio *et al.* (2020) studied the suitable coarsening scale to express an effective hydraulic conductivity. They developed a useful numerical estimator for effective hydraulic conductivity in 2D media.

Among the existing upscaling methods, much attention has been focused on the renormalization approaches because of their reliability and small computational cost. Also, the renormalization can also be modified to detect the preferential flow-paths (Gautier and Noetinger, 1997).

There are relatively few studies in the area of upscaling errors which have not been investigated in detail. Three types of errors which can be caused by upscaling are numerical dispersion, heterogeneity loss and connectivity misrepresentation (Ganjeh-Ghazvini, 2019; Ganjeh-Ghazvini *et al.*, 2015a). The latter mostly occurs in the gas-oil displacement. Due to the low viscosity of the gas, a slight change in the flow paths results in large errors (Ganjeh-Ghazvini *et al.*, 2015b). Preux *et al.* (2016) performed the connectivity analysis based on the shortest paths connecting wells both for a water injection and a gas injection process so as to find an appropriate coarse model. The discrete solution of flow equations leads to numerical error, since only the first few terms of Taylor's series expansion are kept for the approximation of derivative expressions and the rest is neglected. This error exists in both fine and coarse models, but its main indication will be when the model is scaled up and the sizes of the grid blocks become enlarged. Thus, this error highly depends on the block size. In some sources, this classification has been done in a different way; the discretization error (numerical dispersion), heterogeneity loss error and total upscaling error, which is a non-intuitive combination of the two others (Preux, 2016; Sablok and Aziz, 2008).

Heterogeneity shows the intensity of variation in reservoir properties with the location. There is a wide range of tools to produce high-resolution numerical models of reservoir heterogeneities in the petroleum industry (Deutsch and Journel, 1998). These have come from the essential impact of heterogeneity capturing reliable hydrocarbon recovery predictions (Dutton *et al.*, 2003). The heterogeneity can be a result of deposition and/or post-deposition processes e.g., diagenetic, solution, fracture, etc. As a consequence of high variations in permeability and its role in steering the fluid; transport properties are controlled by permeability distribution and their correlations (Hewett, 1986). Hence, understanding the pattern of heterogeneity is critical for the characterization of the connected pores and flow in the subsurface (Alabert and Modot, 1992; Eaton, 2006). Homogenization is a result of upscaling. During the conversion of the fine to coarse model, details such as heterogeneities are lost. The error established due to homogenization is referred to as the heterogeneity loss error (Sablok and Aziz, 2008).

Ganjeh-Ghazvini *et al.* (2015a) studied the relationship between heterogeneity loss and the flow performance error of upscaled models with different upscaling factors. They stated that heterogeneity loss of geological models is influenced by both the overall distribution of permeability values and their arrangements.

In order to perform a reliable flow simulation, it is essential to investigate the parameters that have a significant effect on flow behavior. The relative permeability and mobility ratio play a vital role in fluid distribution. Relative permeability is a cornerstone in multiphase flow simulation and knowledge about the hysteresis and impact of its contrast on flow behavior is essential for three-phase and two-phase flow simulations in Water-Alternating-Gas (WAG) processes, CO_2 sequestration, etc. (Juanes *et al.*, 2006; Spiteri and Juanes, 2006). Many researchers also declared that the pattern of sweep efficiency is very dependent upon the mobility ratio (Aronofsky, 1952; Dyes *et al.*, 1954; Muskat, 1938). Stable or unstable behavior of the water–oil displacement process depends on porous media heterogeneity as well (Durlofsky, 1998; Noetinger *et al.*, 2004). For more information about water–oil upscaling aspects, please refer to Artus and Noetinger (2004).

Up to now, the existing literature on upscaling error focuses particularly on defining the methods of information loss calculation during the upscaling process and developing them. To determine the error due to upscaling, some of this methods only consider the number of cells in fine and coarse grid models; the upscaling factor (Gautier *et al.*, 1999) and upscaling extent parameter (Dasheng, 2010), other methods take the permeability values into account, e.g. data range indicator (Qi and Hesketh, 2004), variance indicator (Preux, 2011), Cardwell and Parsons indicator (Preux, 2016) and the QQ plot (Sablok and Aziz, 2008). Preux (2016) investigated the potential of all mentioned quality indicators to evaluate the information loss. Ganjeh-Ghazvini *et al.* (2015a) introduced a cluster-based method for determining the heterogeneity loss due to upscaling. The advantage of this procedure was taking the overall distribution of permeability values and their spatial arrangements into account, whereas in the previous method they were not considered. Ganjeh-Ghazvini *et al.* (2015b) investigated the connectivity misrepresentation during the upscaling process in a gas injection project. And finally, there is only one study, that is concerned with the direct effect of fluid properties on the error behavior (Ganjeh-Ghazvini, 2019). The author investigated the effect of viscosity contrast on the heterogeneity loss error in an upscaling process.

In this paper, the impact of two very important parameters *i.e.* the relative permeability differences and the mobility ratio on the heterogeneity loss error is studied. This analysis is divided into two steps including investigation of the effect of the relative permeability and the mobility ratio on flow performance.

In this study, the first set of simulation analysis examined the relative permeability contrast and error behavior under this condition. Then, knowing the impact of viscosity and relative permeability ratios separately, their simultaneous impact on the mobility ratio is investigated. For considering the relative permeability contrast, relative permeability ratio (R_p) is defined as:

$$R_p = \frac{K_{rD}^{\max}}{K_{rd}^{\max}}, \tag{1}$$

where $K_{rd}^{\max}$and $K_{rD}^{\max}$ represent the relative permeability of displaced and displacing fluid at the front, respectively. Mobility of a fluid is defined as the relative permeability of a fluid divided by its viscosity. The mobility ratio (M) at the flood-front is described as:

$$M = \frac{K_{rD}^{\max}\mu_d}{K_{rd}^{\max}\mu_D}, \tag{2}$$

$$M = R_p R_v, \tag{3}$$

where, μ_d and μ_D are the displaced and displacing phase viscosity values, respectively and R_v is viscosity ratio and defined as:

$$R_v = \frac{\mu_d}{\mu_D}. \tag{4}$$

The upscaling factor (the level of grid coarsening) is a critical parameter in the simulation process. The higher the upscaling factor is the more fine-scale details may be lost. If this factor is too small, simulations are very time consuming and it is not adequate for implementing different scenarios and realizations of the reservoir. By taking the contrast of relative permeability and mobility into account, one attempt could be the estimation of the optimum level of grid coarsening with respect to the predetermined acceptable value of upscaling error.

This paper deals with the issue that how the heterogeneity loss error behaves at different M and R_p values during the upscaling. In other words, to what extent the fine model can be coarsened to be able to reproduce the fine model behavior relatively accurate under the defined conditions. To capture the effects of the homogenization of coarse models, the reference fine models must be very heterogeneous. For this purpose, the Fractional Brownian Motion (fBm) process is implemented. Then realizations are upscaled by three upscaling factors using the renormalization method. In the next step, the coarse models are refined to the number of the grid blocks of the fine models in order to separate the effect of heterogeneity loss from numerical dispersion. The error of heterogeneity loss of both fine and coarse models is determined by a cluster-based method (Ganjeh-Ghazvini *et al.*, 2015a). The realizations and their corresponding refined models are simulated under waterflooding at three different relative permeability and mobility ratios. The flow performance error is then obtained by comparing the saturation maps of fine and coarse models. Finally, the relation between the flow performance error and heterogeneity loss is investigated and based on that, an upper limit of coarsening is recommended for each analysis beyond which too many details are lost.

2 Methodology

This section is intended to present the simulation model and methodology. It can be illustrated under four steps: fine grid construction, upscaling process, heterogeneity loss calculation based on the clustering method and simulation process. Figure 1 shows the steps utilized for analysis of the heterogeneous loss errors.

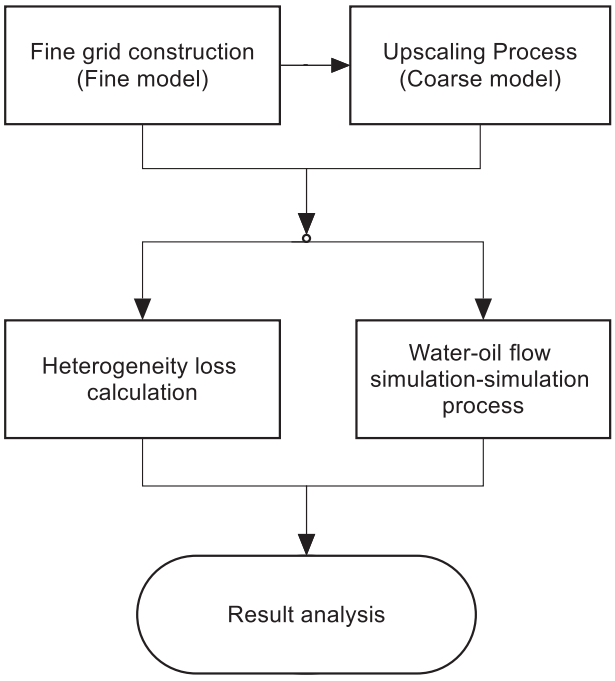

Fig. 1. Illustration of the steps used for heterogeneity loss error analysis.

2.1 Fine grid construction

The first step and prerequisite of any simulation procedure is to have a proper model. In order to obtain the heterogeneity loss of geological maps, the proper model for this investigation is a model with a high degree of heterogeneity which enables us to accurately measure the loss of heterogeneity after the upscaling process.

As it was mentioned, heterogeneity is defined by differences in permeability values. The two-dimensional fBm method is performed to construct the fine grid models. With the discrete Fourier transform, fine grid models can be generated; more details about the procedures can be found in (Ganjeh-Ghazvini *et al.*, 2015b; Hardy and Beier, 1994). The fBm is characterized by the power spectrum of the map that is given below (Hardy and Beier, 1994; Rasaei and Sahimi, 2009):

$$S(\omega) = \frac{a(d)}{\left(\omega_x^2 + \omega_y^2\right)^{H+1}}, \tag{5}$$

where, $S(\omega)$ is the power spectrum, $a(d)$ is the dimensional-dependent constant, ω_x and ω_y present the angular frequency in x and y directions, respectively. The H value is known as the Hurst exponent or the intermittency exponent. When the H is less than 0.5, it implies the negative correlations, which means, the high and low permeability blocks are next to each other. In this paper, the exponent

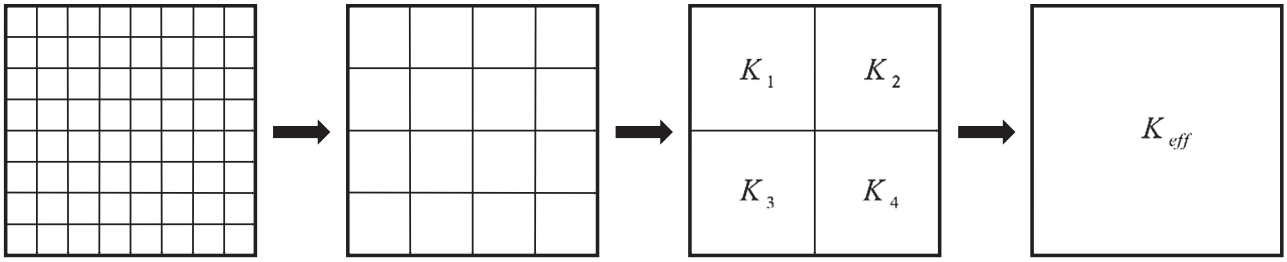

Fig. 2. Algorithm of the renormalization method.

was set to 0.2 to create a very heterogeneous map. The variance is another parameter that could construct a model with a high degree of heterogeneity, as the variance increases, the dispersion of permeability values and its range increases as well. In order to build a map with the mentioned properties, the log-normal distribution of permeability with the mean $\overline{k}_{\ln} = 3$ and variance $\sigma^2_{\ln} = 2.25$ was employed.

2.2 Upscaling process

In order to transform the geological model to the simulation model, the number of grid blocks must, therefore, be reduced by "upscaling". King (1989) has described the real-space renormalization technique based on an electrical analogy for calculating the effective permeability of a heterogeneous medium. The algorithm of this technique starts with 2^{nD} grid blocks. Where n and D are defined as natural numbers and dimensions of realizations, respectively. The number of grid blocks is then reduced to $2^{(n-1)D}$ grid blocks. The effective permeability of each new renormalized block is calculated by:

$$K_{\text{eff}} = \frac{4(K_1 + K_3)(K_2 + K_4) \times A}{A \times (K_1 + K_2 + K_3 + K_4) + 3(K_1 + K_2)(K_3 + K_4)(K_1 + K_3)(K_2 + K_4)}, \tag{6}$$

where:

$$A = [K_2K_4(K_1 + K_3) + K_1K_3(K_2 + K_4)]. \tag{7}$$

The process can be repeated until the desired number of blocks, ultimately one single block is reached as shown in Figure 2.

2.3 Heterogeneity loss calculation based on the clustering method

Numerical dispersion and heterogeneity loss are the upscaling errors in this model. Aiming to investigate the heterogeneity loss separately, the numerical error must be eliminated. For this purpose, the coarse grid blocks could be subdivided into more numbers (Sablok and Aziz, 2008). Ganjeh-Ghazvini *et al.* (2015a) introduced the Refined Upscaled (RU) model, that the RU model has the same size and number of fine grid blocks, whereas, the properties of this model are taken directly from the parent coarse model. The structure and properties of the RU model are shown in Figure 3.

Ganjeh-Ghazvini *et al.* (2015a) introduced a cluster-based method for calculating the level of heterogeneity loss called heterogeneity number. The basis of this method is how the permeability values are arranged and distributed on the map. What it follows is a brief explanation about how the heterogeneity number is determined. First of all, the permeability values are divided into several subintervals by the k-means method, each of these subintervals corresponds to a rock type. In this study, the number of rock types for any realization was determined from the Winland chart (Tavakoli, 2018). Clusters are created from a number of neighboring grid blocks of the same rock type. Two grid blocks are neighbors if they share an edge or a side in 2D or 3D space, respectively. After defining clusters, the coefficient of variation of each cluster is determined by:

$$\text{CV}(C_i) = \left(\frac{\sigma}{\mu}\right)_{\text{over } C_i}, \tag{8}$$

where, σ and μ are the standard deviation and the average of permeability values that belong to the cluster C_i. The intra-cluster heterogeneity number (H_{ac}) measures how different the grid blocks of a cluster are, and is defined as:

$$H_{ac} = \frac{\sum_{c_i} \left(\frac{\sigma}{\mu}\right)_{\text{over } c_i}}{A}, \tag{9}$$

where, A is the area of the model. The dissimilarity between grid blocks of two adjacent clusters is characterized as the inter-cluster heterogeneity. The integrated coefficient of variation $\text{CV}(C_i, C_j)$ is defined as:

$$\text{CV}(C_i, C_j) = \begin{cases} \left(\frac{\sigma}{\mu}\right)_{\text{over } C_i \cup C_j} & \text{if } C_i \text{ and } C_j \text{ are distinct neighboring, clusters} \\ 0 & \text{otherwise,} \end{cases} \tag{10}$$

where, σ and μ are the standard deviation and the average of permeability values that belong to the set of $C_i \cup C_j$. The inter-cluster heterogeneity number (H_{ec}) is calculated as:

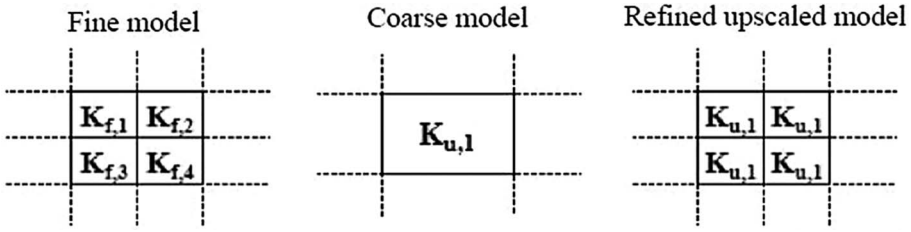

Fig. 3. Grid structure and permeability values for fine, coarse and refined upscaled models (Ganjeh-Ghazvini *et al.*, 2015b).

Table 1. Input parameters for the simulation process.

Parameters	Symbols	Unit	Value
Maximum oil relative permeability	$k_{\mathrm{ro}}^{\max}$	Fraction	1.0
Residual oil saturation	S_{or}	Fraction	0.14
Connate water saturation	S_{wc}	Fraction	0.0
Oil exponent in relative permeability	n_{o}	Dimensionless	3.0
Maximum water relative permeability	$k_{\mathrm{rw}}^{\max}$	Fraction	1.0
Water exponent in relative permeability	n_{w}	Dimensionless	2.0
Oil viscosity	μ_{o}	Centipoise	1.0
Water viscosity	μ_{w}	Centipoise	1.0
Initial pressure	P_i	Psi	1000
Porosity	φ	Fraction	0.2

$$H_{ec} = \frac{\sum_{C_j}\sum_{C_i} \mathrm{CV}(C_i, C_j)}{2A} = \frac{1}{2A}\left\{\left(\frac{\sigma}{\mu}\right)_{C_1 \cup C_2} + \left(\frac{\sigma}{\mu}\right)_{C_1 \cup C_3} + \ldots + \left(\frac{\sigma}{\mu}\right)_{C_{N-1} \cup C_N}\right\}, \quad (11)$$

where N is the total number of clusters.

The heterogeneity number (Ht) is the summation of H_{ac} and H_{ec}:

$$Ht = H_{ac} + H_{ec}. \quad (12)$$

2.4 Simulation process

The injection process that considered in this study was a waterflooding, performed by a common commercial reservoir simulator (Geoquest, 2010) and applied to both fine and coarse models at the same discrete times. In a waterflooding process, water is displacing and oil is the displaced phase.

The realizations were simulated under two different and distinct analysis:

1. Investigate the impact of three different relative permeability ratios *i.e.* 0.5, 1, and 2 on heterogeneity loss error.
2. Investigate the impact of three different mobility ratios *i.e.* 0.1, 1, and 10 on heterogeneity loss error.

The saturation maps of each analysis were prepared, then the saturation error was calculated by detecting the differences between the reference saturation distribution and its corresponding saturation distribution maps of the refined cases at the same discrete times. Root Mean Square Error (RMSE) is the parameter that calculated this difference between two mentioned saturation maps:

$$\mathrm{RMSE} = \sqrt{\frac{\sum_{\mathrm{block}} \left(S_{\mathrm{o,block}}^{f} - S_{\mathrm{o,block}}^{\mathrm{RU}}\right)^2}{N_{\mathrm{total}}^{f}}}, \quad (13)$$

where $S_{\mathrm{o,block}}^{f}$ and $S_{\mathrm{o,block}}^{\mathrm{RU}}$ are the oil saturation in the fine model and refined upscaled model, respectively. N_{total}^{f} is

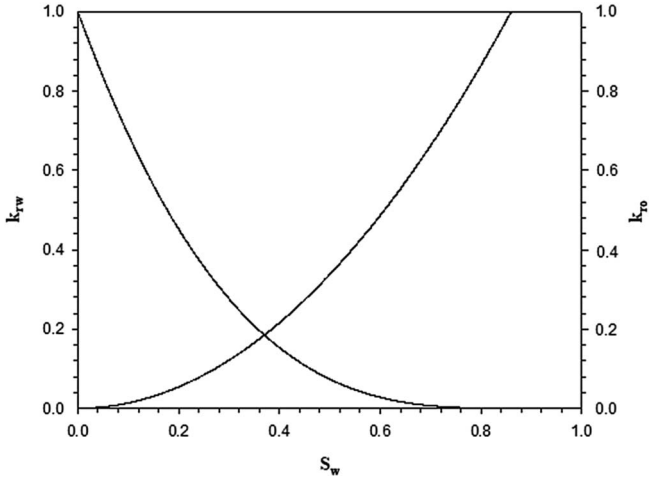

Fig. 4. Water–oil relative permeability curve.

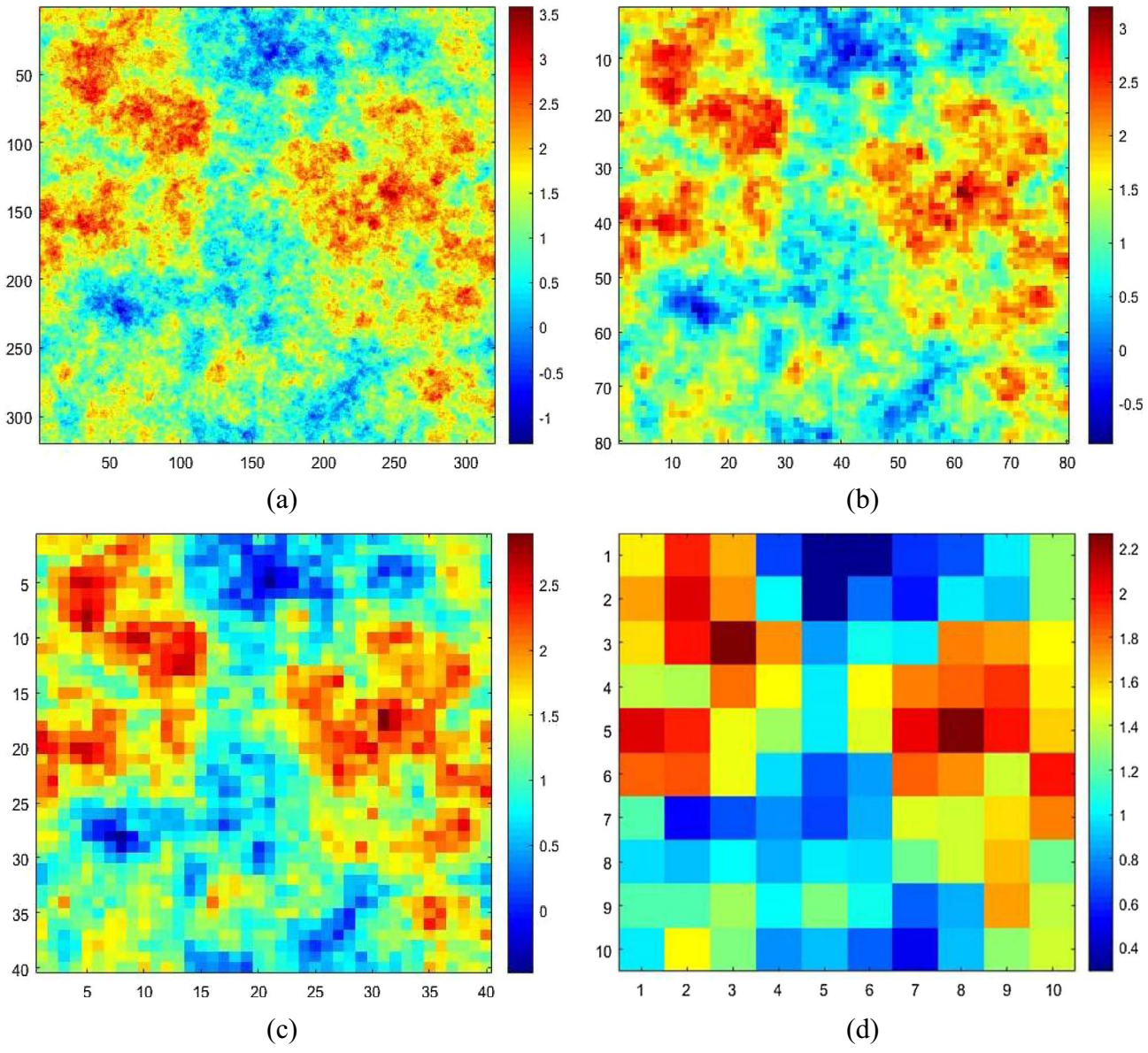

Fig. 5. Permeability distribution map of one realization with logarithmic scale; (a) 320 × 320 fine grid model; (b) 80 × 80 coarse model; (c) 40 × 40 coarse model; and (d) 10 × 10 coarse model.

the total number of grid blocks in the fine model. Flow performance error is determined by the Normalized RMSE (NRMSE) as Ganjeh-Ghazvini *et al.* (2015a):

$$\mathrm{NRMSE} = \frac{\int \frac{\mathrm{RMSE}}{1 - S_{\mathrm{wc}} - \overline{S_{\mathrm{o}}}} \mathrm{d}\overline{S_{\mathrm{o}}}}{\int \frac{1}{1 - S_{\mathrm{wc}} - \overline{S_{\mathrm{o}}}} \mathrm{d}\overline{S_{\mathrm{o}}}}, \tag{14}$$

where, $\overline{S_{\mathrm{o}}}$ and S_{wc} present the volume-waiting average oil saturation of all grid blocks and connate water saturation, respectively.

3 Simulation model

For simulation purposes, 10 realizations were created by the fBm process, which were similar in mean and variance, and different in distribution and range of permeabilities. Each of them contained 320 × 320 × 1 grid blocks with a size of 3.125 × 3.125 × 5 ft in x, y and z-directions, respectively. An injection and a production well with constant rate well mode were located in the first (northwest of the model) and last grid blocks (southeast of the model), respectively. Corey relation was used for determining the oil and water relative permeability values (Corey, 1954):

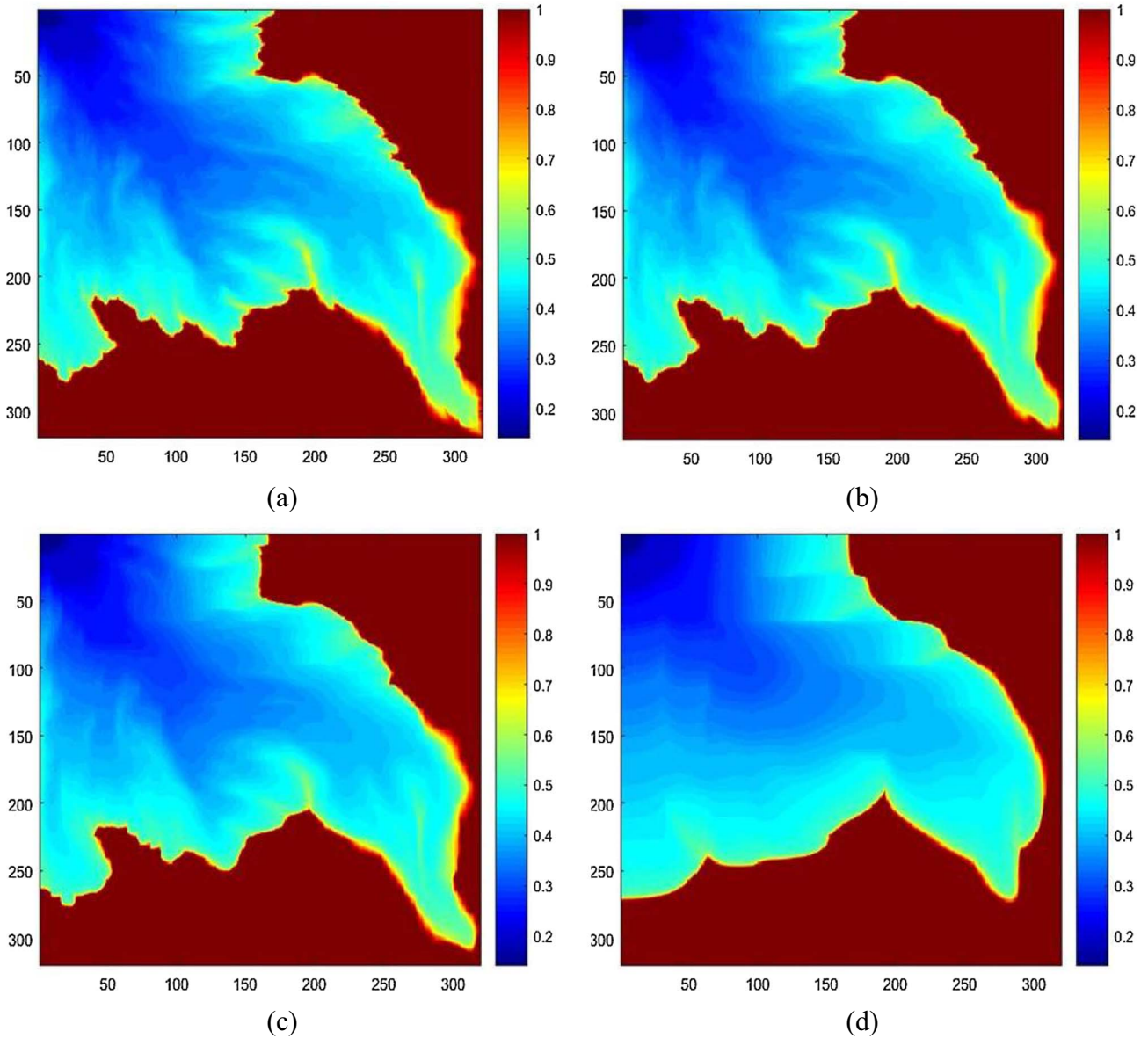

Fig. 6. Oil saturation distribution maps of the fine and corresponding refined upscaled model for one of the realizations at the day of breakthrough; (a) 320 × 320 fine grid model, (b) $RU_{80\times80}$, (c) $RU_{40\times40}$, and (d) $RU_{10\times10}$.

$$k_{\mathrm{ro}} = k_{\mathrm{ro}}^{\max}\left(\frac{S_{\mathrm{o}} - S_{\mathrm{or}}}{1 - S_{\mathrm{or}} - S_{\mathrm{wc}}}\right)^{n_{\mathrm{o}}}, \tag{15}$$

$$k_{\mathrm{rw}} = k_{\mathrm{rw}}^{\max}\left(\frac{S_{\mathrm{w}} - S_{\mathrm{wc}}}{1 - S_{\mathrm{or}} - S_{\mathrm{wc}}}\right)^{n_{\mathrm{w}}}. \tag{16}$$

The fluids were incompressible and capillary pressure was considered to be zero. The other variables used in oil–water displacement simulation are listed in Table 1. Based on equations (15) and (16) and parameters given in Table 1, the relative permeability curve is plotted as shown in Figure 4.

The reference permeability maps were upscaled to different upscaling factors *i.e.*, 4 (80 × 80), 8 (40 × 40) and 32 (10 × 10). Figure 5 displays the permeability distribution for a fine grid realization and its corresponding coarse grid model created by renormalization. Afterward, the refined upscaled models were prepared for the simulation process and heterogeneity loss analysis. The oil–water displacement simulation was performed to the models and all of them were simulated over a specified and equal number of days so as to have an adducible and precise comparison. The number of days was determined based on breakthrough time of realizations when R_p and M are equal to 1. The number of days of the reservoir simulation should not be too low that the breakthrough has not occurred in

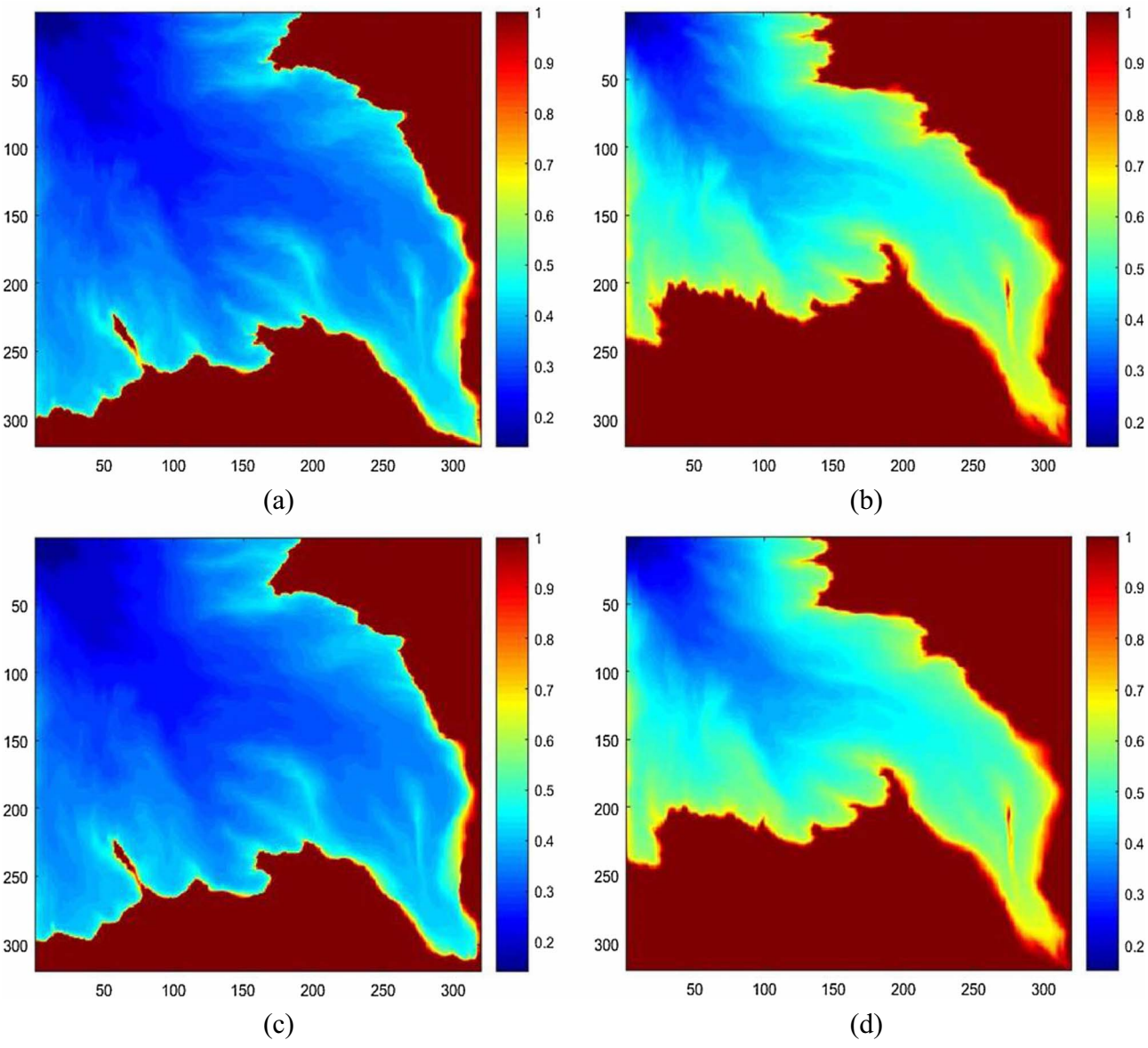

Fig. 7. Comparison of oil saturation maps at $R_p = 0.5$ (a, c, e and g) and $R_p = 2$ (b, d, f and h), (a) and (b) 320 × 320 fine grid model; (c) and (d) $RU_{80\times80}$; (e) and (f) $RU_{40\times40}$; (g) and (h) $RU_{10\times10}$.

the fine grid model and not too high that it has been a long time that the water has arrived in production well. The oil saturation map in fine and RU models for one of the realizations are shown in Figure 6.

4 Results and discussions

As it was mentioned earlier, there is a close relationship between fluid distribution in the porous media and relative permeability and mobility ratio. In this study, we attempted to investigate the effect of relative permeability differences and then, the simultaneous effect of viscosity and relative permeability which appears in mobility ratio on heterogeneity loss error during the upscaling process. Whether the mobility ratio is greater than 1 or not, the heterogeneity loss error leads to a delay in water breakthrough time (Muggeridge *et al.*, 1991). The most favorable displacement mode of the displaced phase by displacing fluid is when the mobility ratio is smaller than one ($M < 1$). Because in this case, the water cannot move faster than the oil and the displacement is carried out in a stable and desirable piston mode. Whereas if the mobility of displacing phase is greater than the displaced one ($M > 1$), then water moves faster than oil and by creating channels in the flow path, which known as fingering, reduces the sweep efficiency of the flooding process relative to the piston state (Allen and Boger, 1988). In this case, the flooding process is unstable and heterogeneity exacerbates this phenomenon. Due to the homogenization of the coarse model which may cause smoother fingers and as a result, the front tracking would be with some errors. Viscous

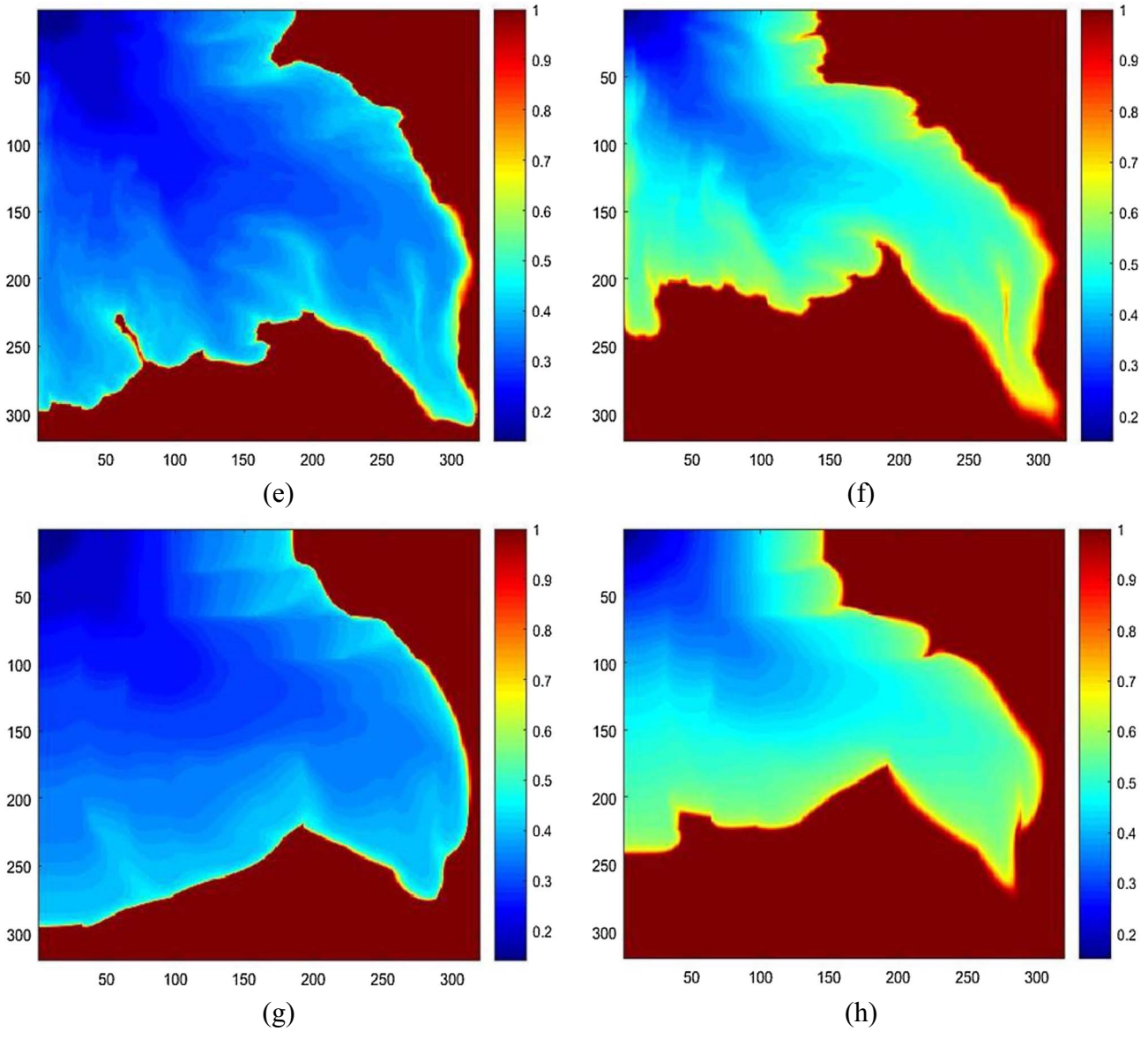

Fig. 7. Continued.

Table 2. The NRMSE values of some refined upscaled models under relative permeability contrast analysis.

Real. no.	$R_p < 1$			$R_p = 1$			$R_p > 1$		
	$RU_{80\times80}$	$RU_{40\times40}$	$RU_{10\times10}$	$RU_{80\times80}$	$RU_{40\times40}$	$RU_{10\times10}$	$RU_{80\times80}$	$RU_{40\times40}$	$RU_{10\times10}$
1	0.0109	0.0219	0.0720	0.0101	0.0208	0.0692	0.0083	0.0179	0.0643
2	0.0106	0.0196	0.0570	0.0102	0.0192	0.0564	0.0087	0.0173	0.0518
3	0.0106	0.0211	0.0531	0.0099	0.0202	0.0519	0.0083	0.0176	0.0468
4	0.0101	0.0218	0.1272	0.0095	0.0206	0.0597	0.0081	0.0181	0.0544

fingering is accentuated by the presence of inhomogeneities, e.g. microscopic heterogeneity (longitudinal dispersion) and, in particular, macroscopic heterogeneity (fracture, channeling) (Tan and Homsy, 1992).

It should be highlighted that the flow performance error (NRMSE) is calculated from the saturation maps after waterflooding simulation. However, the heterogeneity loss is determined based on the absolute permeability discrepancy between blocks and their neighbors or/and clusters. One can conclude that the NRMSE calculates the dynamic error because it is various with time, while the heterogeneity loss error value only depends on the permeability

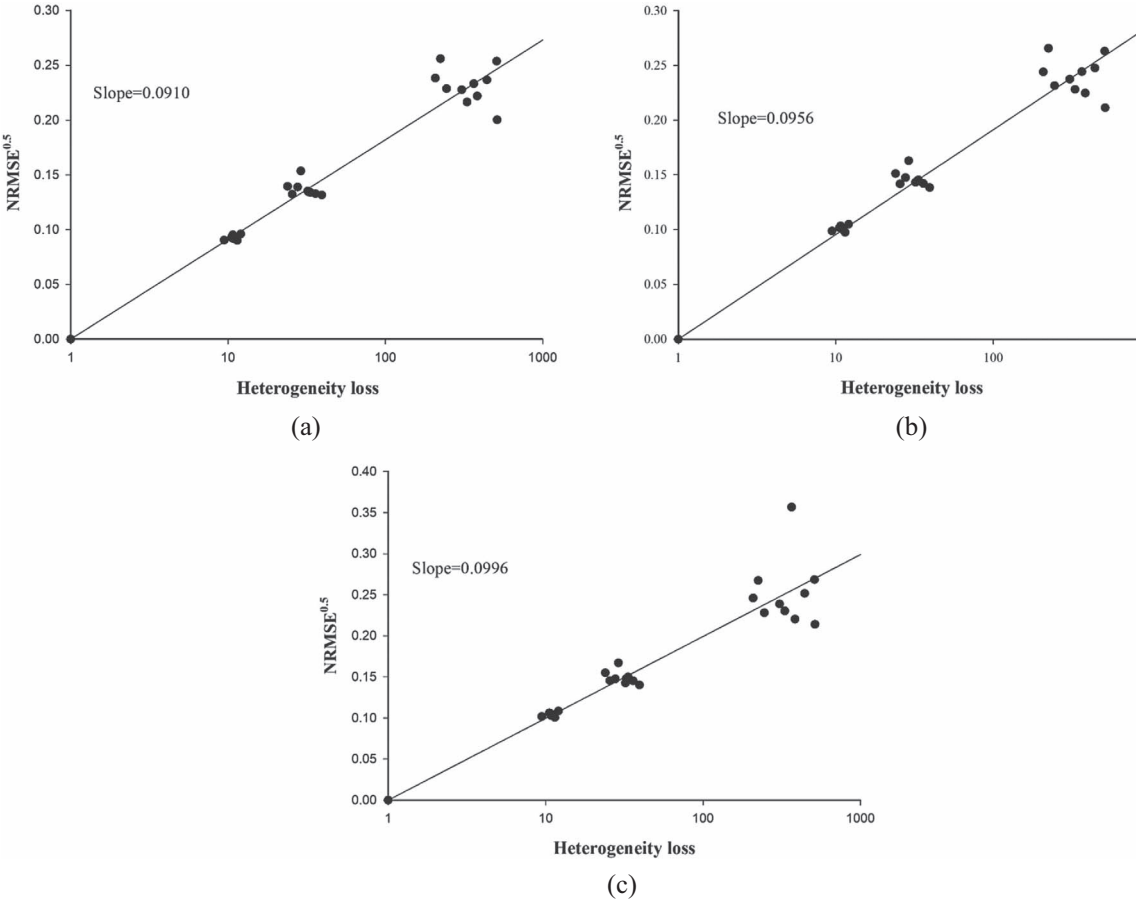

Fig. 8. Heterogeneity loss plot at (a) $R_p > 1$; (b) $R_p = 1$; and (c) $R_p < 1$.

distribution maps in static position regardless of the impact of this distribution on flow behavior. The heterogeneity loss can be calculated at any time that the permeability map (generated by fBm process) is prepared. However, the NRMSE is calculated after the simulation processes.

Heterogeneity loss analysis results in presenting the relationship between the flow performance error (NRMSE) and heterogeneity loss due to the upscaling in a chart, whose slope represents the magnitude of the homogenization error (Ganjeh-Ghazvini *et al.*, 2015a). A more accurate coarse model results in less heterogeneity loss error and a smaller slope. This slope gives us an insight into the advantage of an upscaling method to preserve the heterogeneity over the other methods. Moreover, it also shows how this method behaves under different conditions including fluid properties such as viscosity differences in displaced and displacing phase, and different EOR scenarios such as polymer flooding, WAG, etc. The heterogeneity loss expression is defined as heterogeneity number of the fine model divided by the heterogeneity number of the refined upscaled model $\left(\frac{Ht_f}{Ht_{\mathrm{RU}}}\right)$. The calculation of these heterogeneity numbers was explained before.

4.1 Relative permeability ratio

Relative permeability contrast has a great effect on the fluid distribution and conducting fluids to the production wells (Juanes *et al.*, 2006). Different magnitudes were assigned to the maximum relative permeabilities ($k_{\mathrm{rw}}^{\max}$and $k_{\mathrm{ro}}^{\max}$) to have the desired relative permeability contrast, *i.e.* R_p. Based on the equations (15) and (16) the maximum relative permeability contributes to obtaining the relative permeability values. If $R_p > 1$ which means that the water permeability is more than oil and consequently water fingering is propagated into the system and bypasses the oil to achieve the production well. For the case of $R_p < 1$, which means that the water permeability is less than oil and consequently oil is displaced by water with a favorable relative permeability ratio. In this condition, the observed fronts must be almost flat and piston-like. It should be noted that the presence of the geological heterogeneity has a significant effect on the fluid displacement and the shape of the flood-front. This favorable displacement in comparison with the $R_p > 1$, has a remarkable difference in sweep efficiency as it is shown in Figure 7.

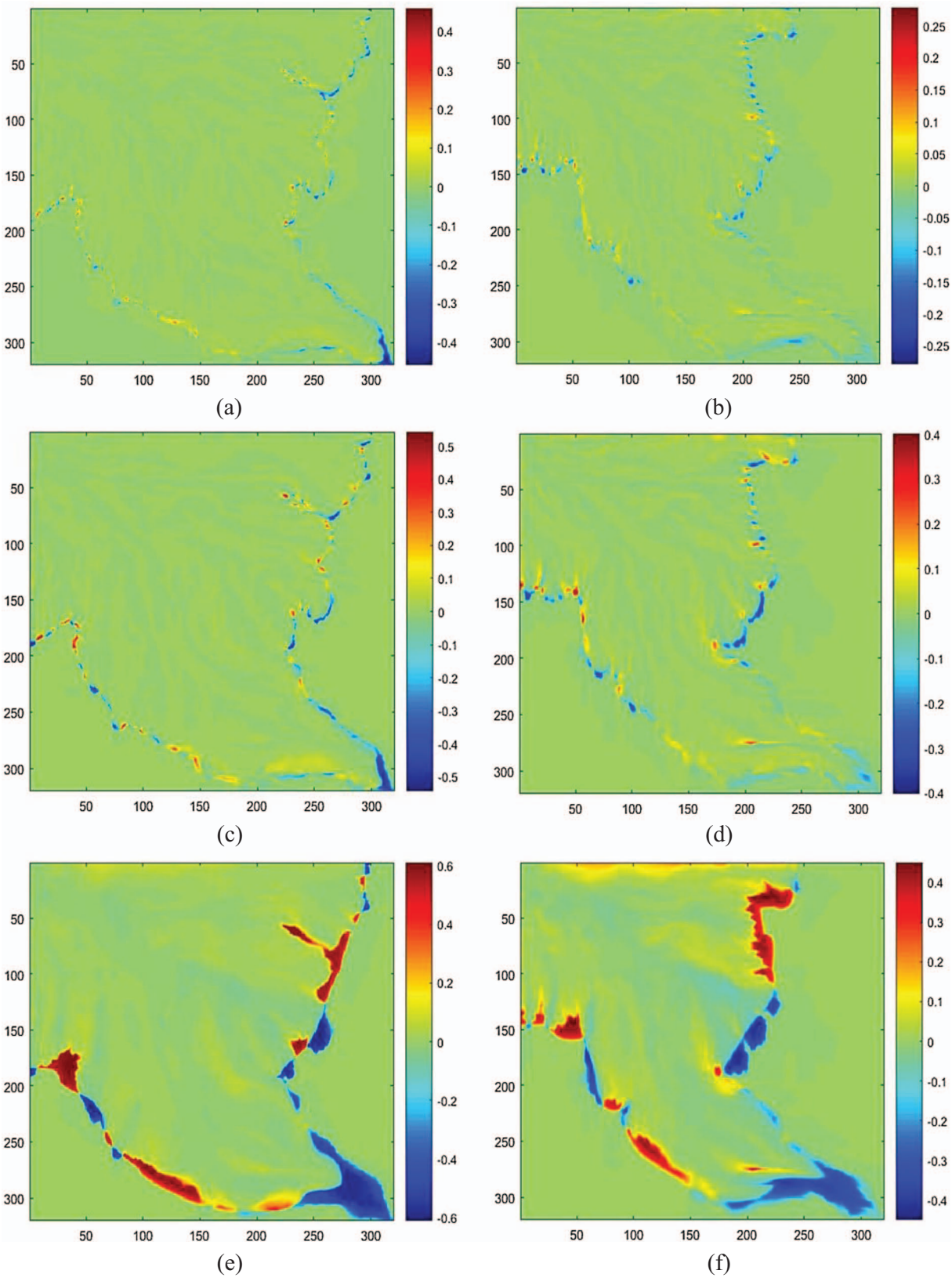

Fig. 9. Oil saturation difference maps between the fine and the RU models at $R_p = 0.5$ (a, c and e) and $R_p = 2$ (b, d and f), (a) and (b) between fine grid model and $RU_{80\times80}$; (c) and (d) between fine grid model and $RU_{40\times40}$; (e) and (f) between fine grid model and $RU_{10\times10}$.

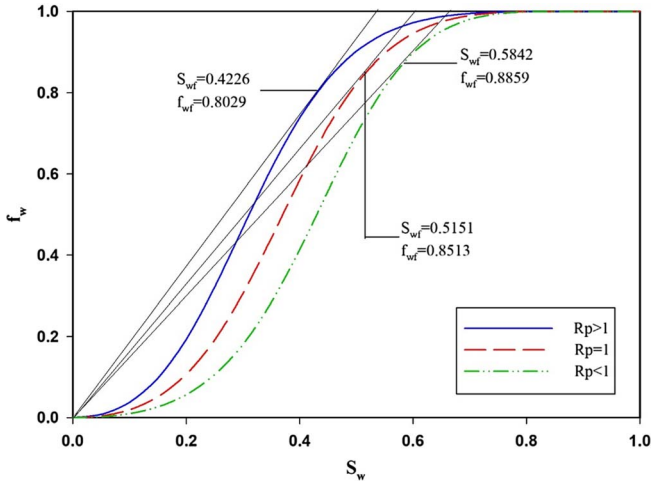

Fig. 10. Fractional flow as a function of saturation for relative permeability analysis, with three different ratios of R_p.

After the simulation process, the saturation map errors were determined. As is shown in Figure 7, the maximum discrepancy between the reference fine model and the corresponding RU models belongs to the grid blocks that flood-front has passed over them recently or the grid blocks around the flood-front. As the water saturation in a certain grid block enhances, the associated error of that block decreases. The place of front highlighted the approximate position of the most errors which varies with time. The NRMSE values of some of the RU models (realizations) are illustrated in Table 2.

In order to perform the heterogeneity loss analysis, the NRMSE *versus* heterogeneity loss was plotted on a semi-log coordinate. Ganjeh-Ghazvini (2019) suggested that a nonlinear trend between the two mentioned parameters such as quadratic seems more appropriate than a linear form. Figure 8 illustrates the root square of NRMSE *versus* heterogeneity loss error for three different ratios of R_p; 0.5, 1 and 2. Based on Table 2 and Figure 8, with decreasing in coarse cell numbers, homogenization occurred in coarse

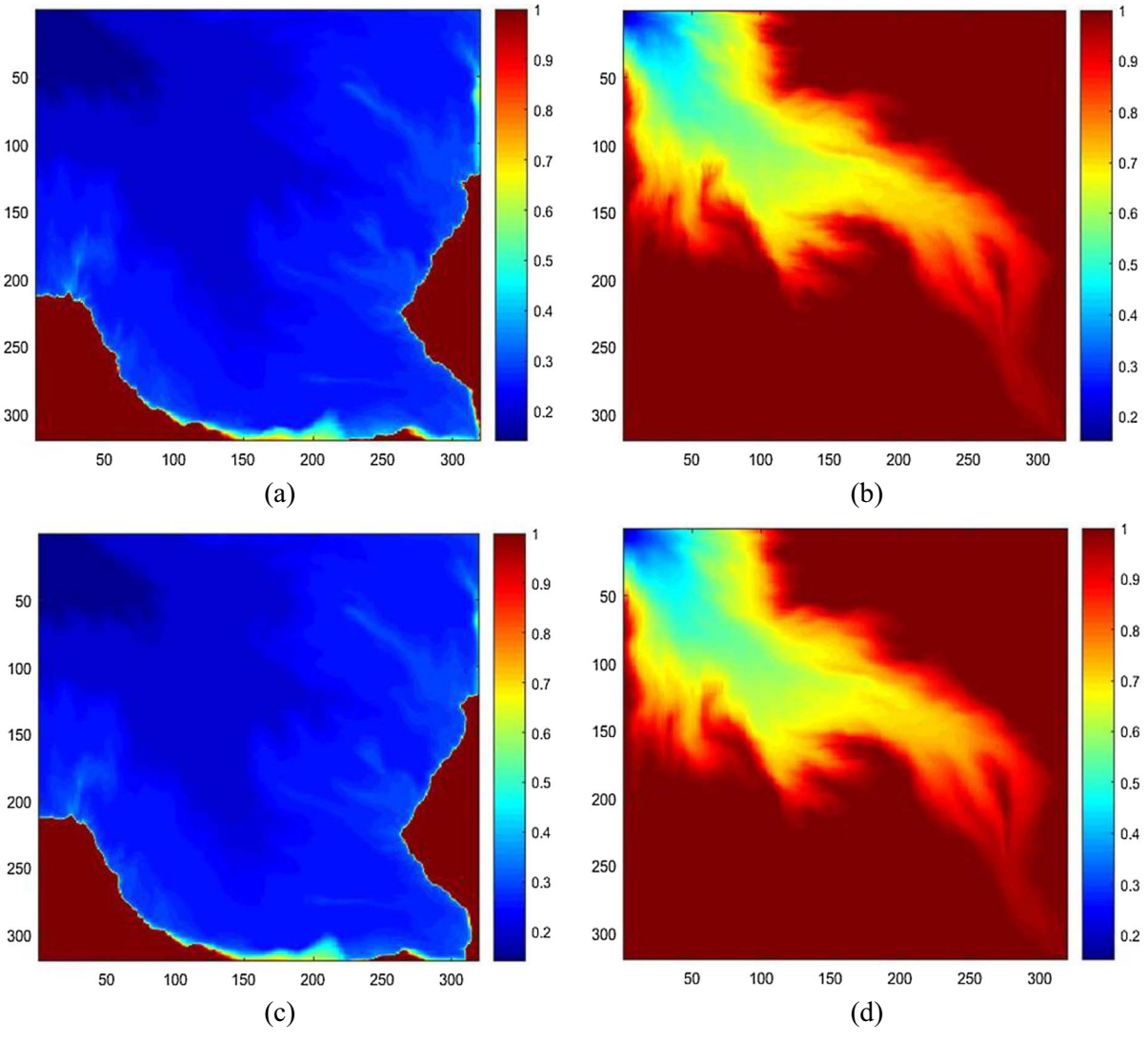

Fig. 11. Comparison of oil saturation maps at $M = 0.1$ (a, c, e and g) and $M = 10$ (b, d, f and h), (a) and (b) 320 × 320 fine grid model; (c) and (d) $RU_{80\times80}$; (e) and (f) $RU_{40\times40}$; (g) and (h) $RU_{10\times10}$.

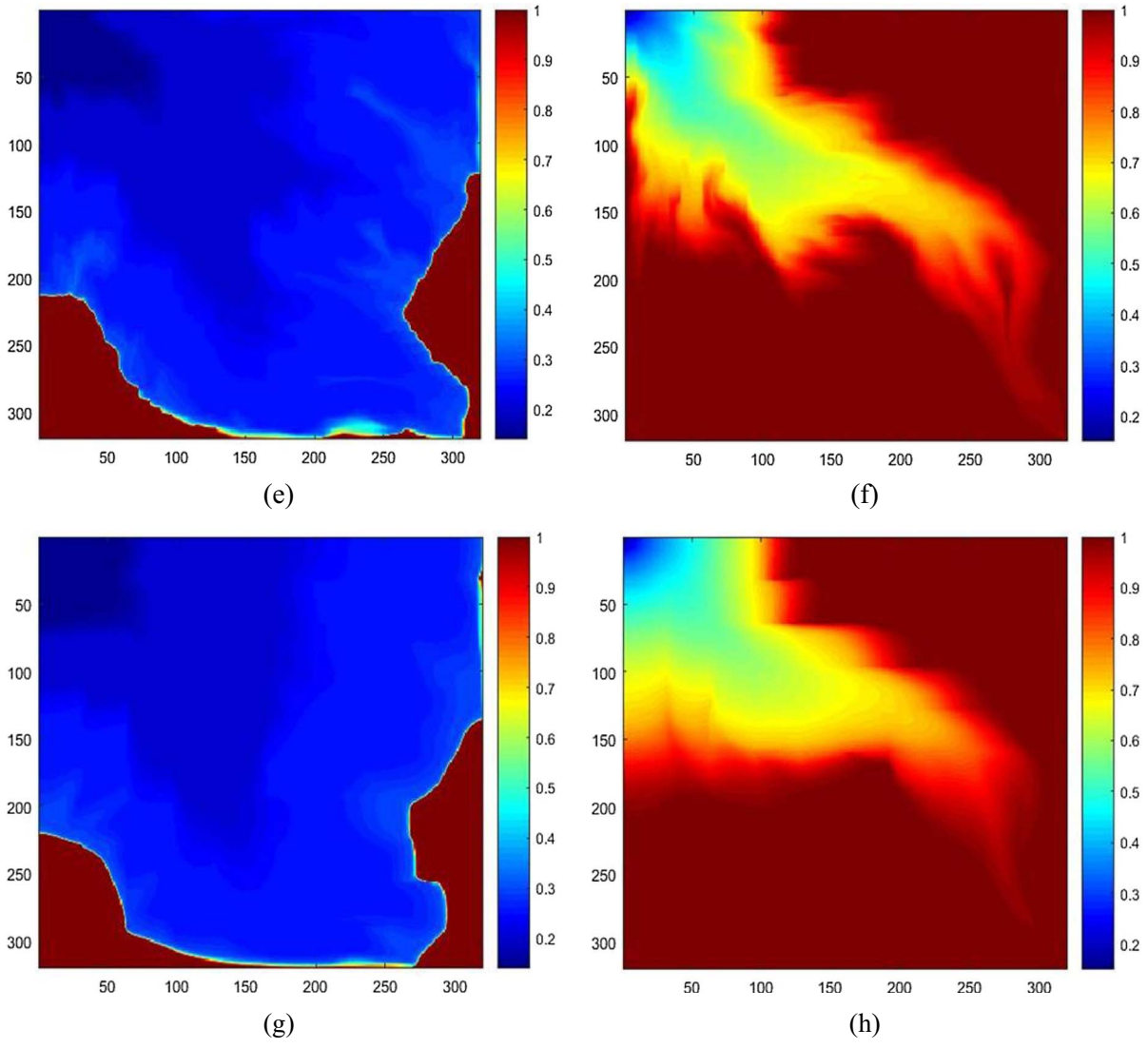

Fig. 11. Continued.

cell models in comparison to the fine-scale heterogeneity. Therefore, the more upscaling factor, the more heterogeneity loss error and NRMSE occurs. With eliminating the heterogeneity in coarse models, the flow cannot distribute in the right paths and it results in more discrepancies between saturation maps and consequently the bigger NRMSE. The slopes for different relative permeability ratios are presented in Figure 8. For the cases of $R_p > 1$, $R_p = 1$ and $R_p < 1$ the slopes of the data are 0.0910, 0.0956 and 0.0996, respectively. The most striking result to emerge from the data, is that the error of $R_p < 1$ is more than those of the $R_p = 1$ and $R_p > 1$. As mentioned earlier, $R_p > 1$ has an unstable front and front tracking in this case is more difficult. Therefore, it is expected that the trend slope of the $R_p < 1$ case should be less than the case of $R_p > 1$. This anomaly can be justified by the source of determination of flow performance error, comparison of the S_o map of the fine and corresponding RU models and eventually by the concept of saturation of displacing phase at the front.

For a reasonable explanation of the error behavior at the mentioned ratios, we investigated the source of error. In heterogeneity loss analysis, the flow performance error is described by NRMSE which is a function of RMSE. The RMSE (Eq. (13)) is determined based on the average difference of the saturation values between the fine and the RU models. A comparison of the saturation maps seems to be useful. Figure 9 illustrates the oil saturation difference maps between the fine and the RU models shown in Figure 7. From the error range given, it can be seen that in some areas, the front in RU models has been estimated ahead of (positive values) or behind (negative values) the accurate front location. These variations depend on the blocks' positions relative to the front location. Hence, grid blocks do not have the same contribution to the error.

As it is shown in Figure 9, with a little imprecision in front locating by RU models, a great saturation difference has happened which caused a great flow performance error. This error could be more significant especially with the

Table 3. The NRMSE values of some refined upscaled models under mobility ratio analysis.

Real. no.	$M < 1$			$M = 1$			$M > 1$		
	$RU_{80\times80}$	$RU_{40\times40}$	$RU_{10\times10}$	$RU_{80\times80}$	$RU_{40\times40}$	$RU_{10\times10}$	$RU_{80\times80}$	$RU_{40\times40}$	$RU_{10\times10}$
1	0.0100	0.0204	0.0704	0.0093	0.0193	0.0644	0.0040	0.0092	0.0416
2	0.0095	0.0183	0.0517	0.0094	0.0178	0.0513	0.0047	0.0095	0.0308
3	0.0098	0.0195	0.0479	0.0097	0.0186	0.0473	0.0038	0.0089	0.0248
4	0.0100	0.0216	0.0575	0.0088	0.0191	0.0537	0.0039	0.0086	0.0308

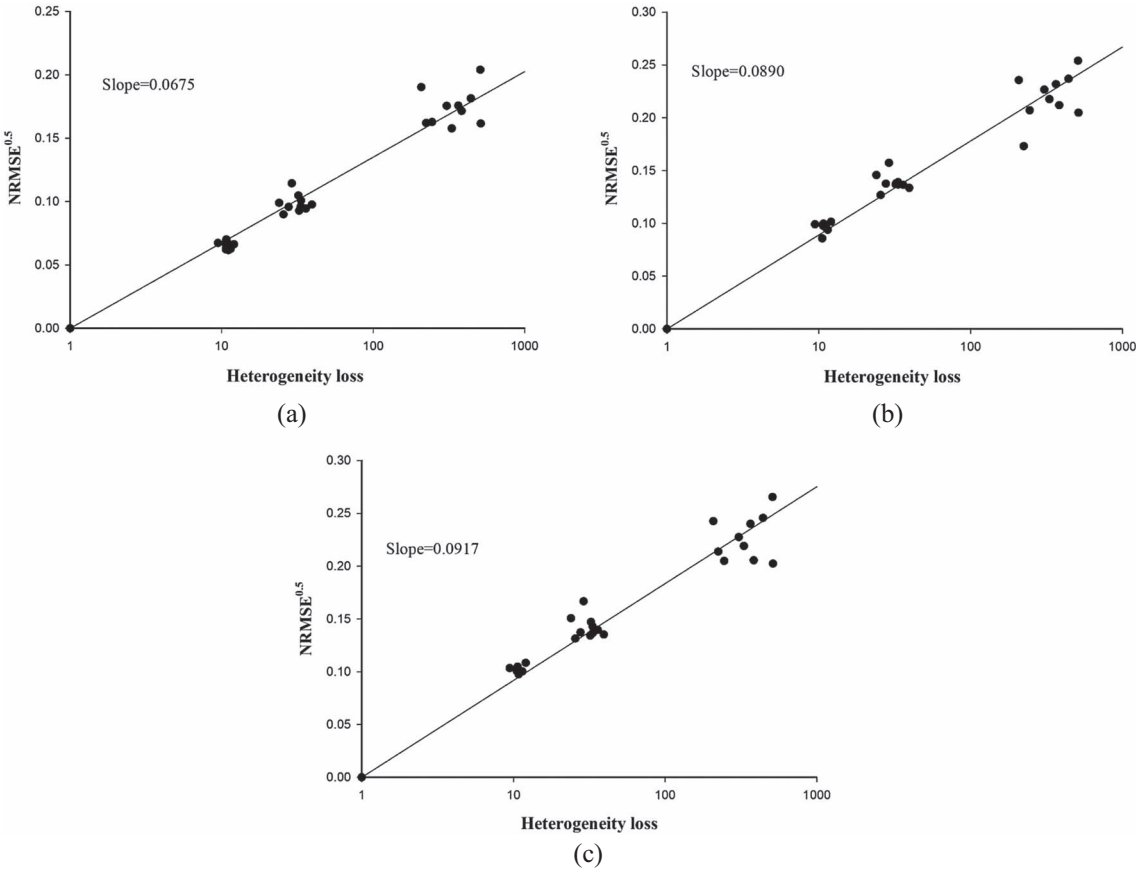

Fig. 12. Heterogeneity loss plot at (a) $M > 1$; (b) $M = 1$; (c) $M < 1$.

presence of high saturation of displacing phase at the front (S_{Df}). The frontal advanced theory was introduced by Buckley and Leverett (1942) to explain the fluid displacement mechanism in sandstone reservoirs. By neglecting the gravity forces and capillary pressure differences in a horizontal system, the fraction of displacing fluid can be computed from equation (17):

$$f_D = \frac{\frac{k_{rD}}{\mu_D}}{\frac{k_{rD}}{\mu_D} + \frac{k_{rd}}{\mu_d}}, \tag{17}$$

where f_D is the fractional flow of the displacing phase.

The relative permeability diagrams for all three ratios are available, based on these diagrams and equation (17), the fractional flows of water, f_w, were calculated and their changes are depicted in Figure 10. In the light of the frontal advance theory, it can be seen why the realizations with $R_p < 1$ suffer from the bigger NRMSE values than those of the $R_p > 1$. By increasing in R_p, the f_w diagram shifts to the right. Consequently, the water fractional flow at the front (f_{wf}) and proportionally the S_{wf} are decreased. In the case of $R_p = 0.5$ with the greatest S_{wf}, a slight failure in front locating may cause a significant error. Whereas, for $R_p = 2$ although the heterogeneity loss and viscous fingering lead to a union against the detection of front location, the lower S_{wf} results in smaller slope as a result of smaller NRMSE values.

One of the main concerns of any petroleum engineer to simulate a reservoir is a suitable choice for the type or level of upscaling. The degree of coarsening cannot be too high due to the loss in detail such as heterogeneity and numerical dispersion. Besides, the simulation of a geological fine grid model or a model with a very low upscaling factor will be

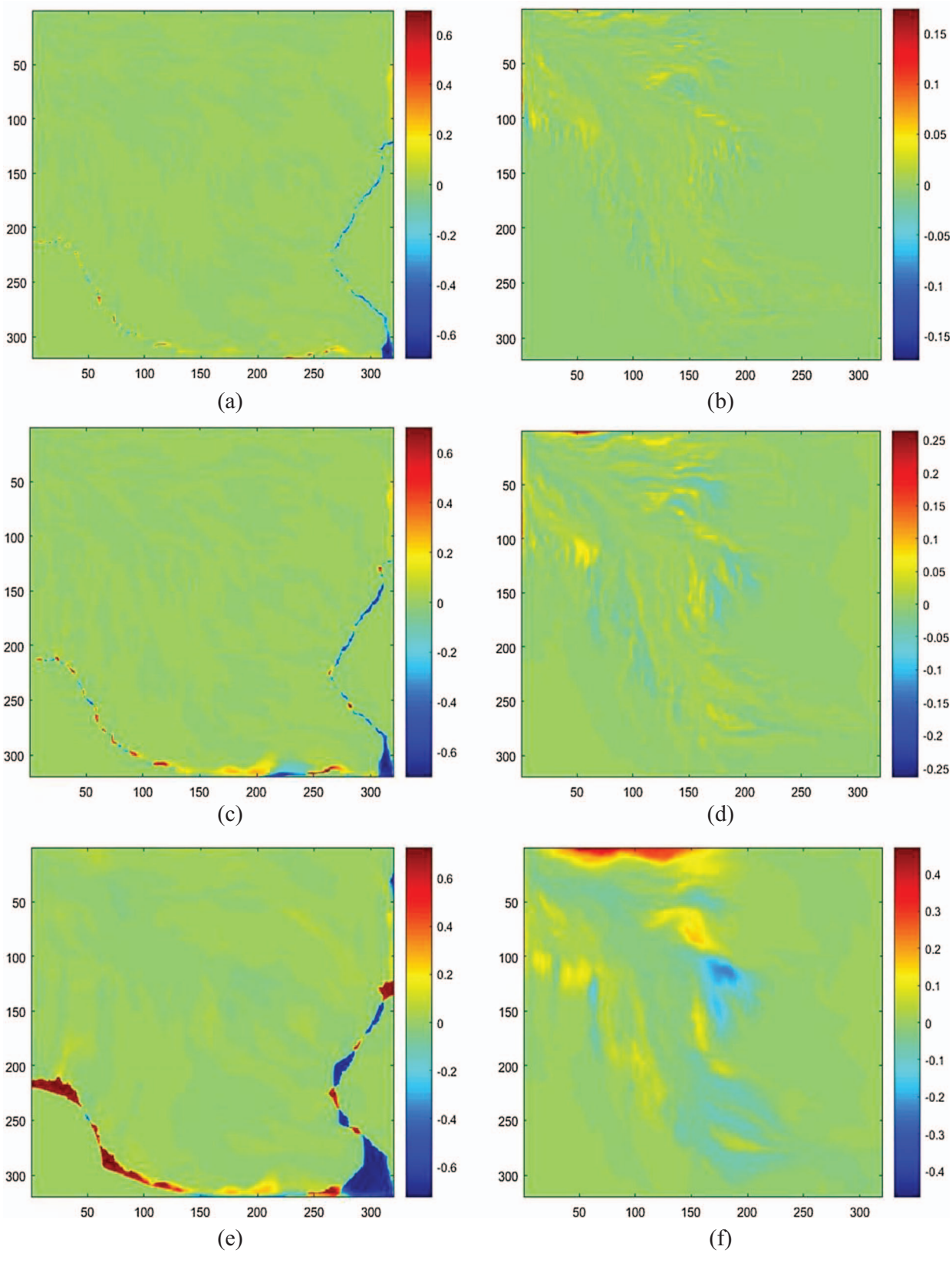

Fig. 13. Oil saturation difference maps between the fine and the RU models at $M = 0.1$ (a, c and e) and $M = 10$ (b, d and f), (a) and (b) between fine grid model and $RU_{80\times80}$; (c) and (d) between fine grid model and $RU_{40\times40}$; (e) and (f) between the fine grid model and $RU_{10\times10}$.

impractical and time-consuming given the scenarios ahead as well as the hardware constraint. Based on the relation between the square root of NRMSE and heterogeneity loss error, an upper limit of coarsening can be obtained from the slope of each ratio, provided that the numerical dispersion is sufficiently small. In this manner, a pre-known value of NRMSE is employed which is an acceptable error value with accurate results in coarse models. The upper limit of coarsening is an approximate value (as in this research, the effect of numerical error is eliminated to investigate the heterogeneity loss behavior), unless the numerical dispersion would be very small and/or diminishes someway or the total upscaling error would have been reduced due to the opposing nature of these two types of errors (Preux, 2016; Sablok and Aziz, 2008). To have a reasonable result, the NRMSE should not exceed of 0.085 (Ganjeh-Ghazvini *et al.*, 2015a). Based on the slopes shown in Figure 8 and the critical value of NRMSE, the results of a coarse model are trustworthy if the ratio of $\left(\frac{Ht^f}{Ht^{RU}}\right)$ does not exceed from 1598, 1121 and 845 for $R_p = 2$, $R_p = 1$ and $R_p = 0.5$, respectively. This approach gives us the critical heterogeneity loss ratio, not the number of grid blocks or size of them. The fine models are upscaled by several various upscaling factors, the coarse block that has the biggest heterogeneity loss number before reaching the critical value is the most appropriate one. More erroneous results are produced at relative permeability ratios less than unity. Therefore, the closer the shape of the front to the piston-shape is, the greater the errors as well as the lower the optimum quantity of upscaling factor become. For the accurate simulation in water-wet reservoirs where water relative permeability is less than oil relative permeability, either coarse grid blocks should be small enough or a more robust method is employed for upscaling purposes.

4.2 Mobility ratio

Another parameter that can lead to a significant effect on the flow distribution is the mobility ratio. Three different ratios were considered to study the effect of mobility ratio on heterogeneity loss error including $M = 10$, 1 and 0.1. For $M = 10$ ($M > 1$), the mobility of the displacing phase (water) is 10 times more than the displaced phase (oil). Therefore, the water will achieve the production well really soon by bypassing the oil and resulted in a week sweep efficiency. In this case, the heterogeneity loss and viscous fingering together were caused a significant error due to the disability to follow the exact flood-front of the fine model. In the ratio of $M = 0.1$, the displacing phase pushed the oil to the production well with a significant sweep efficiency. The front tracking is much easier as it is shown in Figure 11.

To determine the heterogeneity loss error affected by the different values of mobility ratio, the waterflooding simulation was performed. Then the NRMSE was calculated by comparing the oil saturation values of the fine and the refined upscaled model. The results are reported in Table 3. Finally, the square root of NRMSE ($\sqrt{\text{NRMSE}}$) *versus* heterogeneity loss for all upscaling factors and mobility ratios are plotted in a semi-log graph as shown in Figure 11. The NRMSE values in Table 3 and Figure 12 illustrate that an increase in mobility ratio results in a decrease in flow performance error. Whereas, exactly the opposite trend is expected to happen. The distribution maps of the errors are demonstrated in Figure 13.

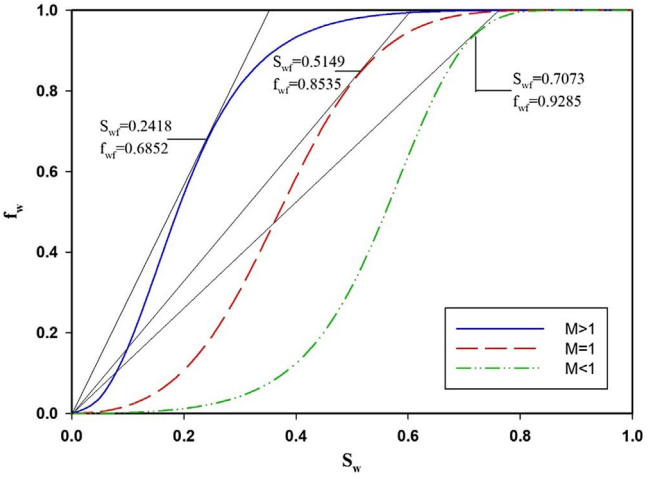

Fig. 14. Fractional flow as a function of saturation for relative permeability analysis, with three different ratios of M.

The water fractional flow *versus* water saturation is plotted in Figure 14 in the same way as explained in the previous section. As discussed earlier, based on the frontal-advance theory, the error behavior can be justified as shown in Figure 14. In the following, according to the slopes of each ratio which shown in Figure 12 and the critical value of NRMSE, the ratio of $\left(\frac{Ht^f}{Ht^{RU}}\right)$ of a proper coarse model for development projects should not exceed from 20 855, 1887, and 1511 for $M = 10$, $M = 1$ and $M = 0.1$, respectively. The number of grid blocks cannot be obtained directly from this approach, because it gives us the heterogeneity loss ratio but based on this value the proper number of coarse grid blocks can be easily obtained. Knowledge about the impacts of fluid properties on upscaling errors is useful in implementing a more effective method for upscaling in more sensitive reservoirs. More caution should be given to piston-shaped water fronts in other words to reservoirs with $M < 1$. To achieve the specified heterogeneity loss ratio, one must either need to manipulate its upscaling factor or use a more potent upscaling method.

5 Conclusion

In this paper, we have investigated the impact of relative permeability contrast and mobility ratio on heterogeneity loss error due to the upscaling process. The main findings can be summarized as follows:

1. By comparing the oil saturation maps of fine and corresponding refined upscaled models, it is clear that most of the NRMSE happen in blocks nearby the

front. As the front goes by through the blocks, the error is increased and by taking some distance of them the error will be reduced. This finding confirms that a non-uniform coarsening method which changes with time can aid in the progress of the accurate front tracking.

2. The results illustrate that the heterogeneity loss error is more significant when the relative permeability ratio is less than one ($R_p < 1$). In a consequence, the level of upscaling for reservoirs which has a lower relative permeability of displacing phase than the displaced one (for example this could happen in reservoirs with favorable wettability for displacing phase), must be small enough. Or, a more powerful upscaling method should be used such that the error does not exceed the critical value.

3. Characterization of the impact of parameters such as relative permeability and mobility ratio is essential for our increased understanding of the optimum level of upscaling process. In heavy oil reservoirs with oil-wet natures where oil cannot be displaced easily in a piston shape with mobility ratio more than one, sensitivities to the choice of the coarse grid block sizes are less. As a result, production forecasts can be done with a lot of time-saving and an acceptable level of accuracy. In comparison, water-wet reservoirs with light oil are more sensitive, so it should be done with more caution in choosing the level of upscaling and/or hiring a more powerful upscaling method. In EOR processes like polymer injection in which M is less than unity and front is piston-like, in comparison to injection a lighter fluid, a more robust upscaling method or less upscaling factor should be employed.

References

Aarnes J.E., Kippe V., Lie K.A. (2005) Mixed multiscale finite elements and streamline methods for reservoir simulation of large geomodels, *Adv. Water Resour.* **28**, 3, 257–271. doi: 10.1016/j.advwatres.2004.10.007.

Alabert F.G., Modot V. (1992) Stochastic models of reservoir heterogeneity: Impact on connectivity and average permeabilities, in: *67th Annual Technical Conference and Exhibition of the Society of Petroleum Engineers held in Washington, DC, October 4–7, 1992*, pp. 355–370. doi: 10.2118/24893-MS.

Allen E., Boger D.V. (1988) The influence of rheological properties on mobility control in polymer-augmented waterflooding, in: *63rd Annual Technical Conference and Exhibition of the Society of Petroleum Engineers held in Houston, TX, October 2–5, 1988*, pp. 449–456. doi: 10.2118/18097-MS.

Aronofsky J.S. (1952) Mobility ratio – its influence on flood patterns during water encroachment, *J. Pet. Technol.* **4**, 1, 15–24. doi: 10.2118/132-g.

Artus V., Noetinger B. (2004) Up-scaling two-phase flow in heterogeneous reservoirs : Current trends, *Oil Gas Sci. Technol. - Rev. IFP Energies nouvelles* **59**, 2, 185–195.

Audigane P., Blunt M.J. (2004) Dual mesh method for upscaling in waterflood simulation, *Transp. Porous Media* **55**, 1, 71–89. doi: 10.1023/B:TIPM.0000007309.48913.d2.

Barker J.W., Thibeau S. (1997) A critical review of the use of pseudorelative permeabilities for upscaling, *SPE Reserv. Eng.* **12**, 2, 138–143. doi: 10.2118/35491-PA.

Buckley S.E., Leverett M.C. (1942) Mechanism of fluid displacement in sands, *Trans. AIME* **146**, 1, 107–116. doi: 10.2118/942107-g.

Chen Z. (2007) *Reservoir simulation: Mathematical techniques in oil recovery*, Society for industrial and applied mathematics, Calgari, Alberta, Canada, pp. 1–6. doi: 10.1137/1.9780898717075.ch1.

Chen Y., Durlofsky L.J. (2006) Adaptive local – global upscaling for general flow scenarios in heterogeneous formations, *Transp. Porous Media* **62**, 157–185. doi: 10.1007/s11242-005-0619-7.

Christie M.A. (1996) Upscaling for reservoir simulation, *J. Pet. Technol.* **48**, 11, 1004–1010. doi: 10.2118/37324-JPT.

Christie M.A., Wallstrom T.C., Durlofsky L.J., Sharp D.H., Zou Q. (2007) Effettive medium boundary conditions in upscaling, *Los Alamos National Laboratory Technical Report LA-UR-00-2804*. doi: 10.3997/2214-4609.201406146.

Colecchio I., Boschan A., Otero A.D., Noetinger B. (2020) On the multiscale characterization of effective hydraulic conductivity in random heterogeneous media: a historical survey and some new perspectives, *Adv. Water Resour.* **140**, 103594. doi: 10.1016/j.advwatres.2020.103594.

Corey A.T. (1954) The interrelation between gas and oil relative permeabilites, *Prod. Mon.* **19**, 1, 38–41.

Darman N.H., Pickup G.E., Sorbie K.S. (2002) A comparison of two-phase dynamic upscaling methods based on fluid potentials, *Comput. Geosci.* **6**, 1, 5–27. doi: 10.1023/A:1016572911992.

Dasheng Q. (2010) Upscaling extent vs. information loss in reservoir upscaling, *Pet. Sci. Technol.* **28**, 12, 1197–1202. doi: 10.1080/10916460903057865.

Deutsch C., Journel A. (1998) *GSLIB Geostatistical Software Library and User's Guide Second Edition*, Oxford University Press.

Durlofsky L.J. (1998) Coarse scale models of two phase flow in heterogeneous reservoirs: Volume averaged equations and their relationship to existing upscaling techniques, *Comput. Geosci.* **2**, 73–92.

Durlofsky L.J. (2003) Upscaling of geocellular models for reservoir flow simulation: A review of recent progress, in: *7th International Forum on Reservoir Simulation Buhl/Baden-Baden, Germany, June 23–27, 2003*, pp. 1–58.

Durlofsky L.J. (2005) Upscaling and gridding of fine scale geological models for flow simulation, in: *8th International Forum on Reservoir Simulation Iles Borromees, Stresa, Italy*, pp. 1–59.

Dutton S.P., Flanders W.A., Barton M.D. (2003) Reservoir characterization of a Permian deep-water sandstone, East Ford field, Delaware Basin, Texas, *Am. Assoc. Pet. Geol. Bull.* **87**, 4, 609–627. doi: 10.1306/10100201085.

Dyes A.B., Caudle B.H., Erickson R.A. (1954) Oil production after breakthrough as influenced by mobility ratio, *J. Pet. Technol.* **6**, 4, 27–32. doi: 10.2118/309-g.

Eaton T.T. (2006) On the importance of geological heterogeneity for flow simulation, *Sediment. Geol.* **184**, 3–4, 187–201. doi: 10.1016/j.sedgeo.2005.11.002.

Ertekin T., Abou-Kassem J., King G. (2001) Basic applied reservoir simulation, in: A. Spivak, J.E. Killough (eds), *SPE*, Richardson, Texas, pp. 1–8.

Ganjeh-Ghazvini M. (2019) The impact of viscosity contrast on the error of heterogeneity loss in upscaling of geological models, *J. Pet. Sci. Eng.* **173**, 681–689. doi: 10.1016/j.petrol.2018.10.061.

Ganjeh-Ghazvini M., Masihi M., Baghalha M. (2015a) Effect of connectivity misrepresentation on accuracy of upscaled models in oil recovery by CO_2 injection, *Greenh. Gases Sci. Technol.* **6**, 339–351. doi: 10.1002/ghg.

Ganjeh-Ghazvini M., Masihi M., Baghalha M. (2015b) Study of heterogeneity loss in upscaling of geological maps by introducing a cluster-based heterogeneity number, *Physica A* **436**, 1–13. doi: 10.1016/j.physa.2015.05.010.

Gautier Y., Noetinger B. (1997) Preferential flow-paths detection for heterogeneous reservoirs using a new renormalization technique, *Transp. Porous Media* **26**, 1, 1–23.

Gautier Y., Blunt M.J., Christie M.A. (1999) Nested gridding and streamline-based simulation for fast reservoir performance prediction, *Comput. Geosci.* **3**, 3–4, 295–320. doi: 10.2523/51931-ms.

Geoquest. (2010) *Eclipse 100 reference manual*, Schlumberger.

Hardy H.H., Beier R.A. (1994) *Fractals in reservoir engineering*, World Scientific.

Hewett T.A. (1986) Fractal distributions of reservoir heterogeneity and their influence on fluid transport, in: *61st Annual Technical Conference and Exhibition of the Society of Petroleum Engineers, New Orieans, LA, October 5–8, 1986.* doi: 10.2118/15386-MS.

Holden L., Nielsen B.F. (2000) Global upscaling of permeability in heterogeneous reservoirs; the Output Least Squares (OLS) method, *Transp. Porous Media* **40**, 2, 115–143. doi: 10.1023/A:1006657515753.

Juanes R., Spiteri E.J., Orr F.M., Blunt M.J. (2006) Impact of relative permeability hysteresis on geological CO_2 storage, *Water Resour. Res.* **42**, 12, 1–13. doi: 10.1029/2005WR004806.

Karimi-Fard M., Durlofsky L.J. (2016) A general gridding, discretization, and coarsening methodology for modeling flow in porous formations with discrete geological features, *Adv. Water Resour.* **96**, 354–372. doi: 10.1016/j.advwatres.2016.07.019.

King P.R. (1989) The use of renormalization for calculating effective permeability, *Transp. Porous Media* **4**, 1, 37–58. doi: 10.1007/BF00134741.

Kyte J.R., Berry D.W. (1975) New pseudo functions to control numerical dispersion, *Soc. Pet. Eng. AIME J.* **15**, 4, 269–276. doi: 10.2118/5105-pa.

Liao Q., Lei G., Zhang D., Patil S. (2019) Analytical solution for upscaling hydraulic conductivity in anisotropic heterogeneous formations, *Adv. Water Resour.* **128**, 97–116. doi: 10.1016/j.advwatres.2019.04.011.

Matthai S.K., Nick H.M. (2009) Upscaling two-phase flow in naturally fractured reservoirs, *Am. Assoc. Pet. Geol. Bull.* **93**, 11, 1621–1632. doi: 10.1306/08030909085.

Misaghian N., Assareh M., Sadeghi M.T. (2018) An upscaling approach using adaptive multi-resolution upgridding and automated relative permeability adjustment, *Comput. Geosci.* **22**, 1, 261–282. doi: 10.1007/s10596-017-9688-2.

Muggeridge A.H., Lake L.W., Carroll H.B., Wesson T.C. (1991) Generation of effective relative permeabilities from detailed simulation of flow in heterogeneous porous media, in: *Reservoir characterization II*, pp. 197–225.

Muskat M. (1938) The flow of homogeneous fluids through porous media, *Soil Sci.* **46**, 2, 169.

Noetinger B., Artus V., Ricard L. (2004) Dynamics of the water – oil front for two-phase, immiscible flow in heterogeneous porous media. 2 – isotropic Media, *Transp. Porous Media* **56**, 3, 305–328.

Peaceman D.W. (1997) Effective transmissibilities of a gridblock by upscaling-Comparison of direct methods with renormalization, *SPE J.* **2**, 3, 338–349. doi: 10.2118/36722-PA.

Pickup G.E., Ringrose P.S., Corbett P.W.M., Jensen J.L., Sorbie K.S. (1995) Geology, geometry and effective flow, *Pet. Geosci.* **1**, 1, 37–42. doi: 10.1144/petgeo.1.1.37.

Preux C. (2011) Study of evaluation criteria for reservoir upscaling, in: *73rd EAGE Conference & Exhibition Incorporating SPE EUROPEC, Vienna, Austria, 23–26 May.* doi: 10.3997/2214-4609.20149454.

Preux C. (2016) About the use of quality indicators to reduce information loss when performing upscaling, *Oil Gas Sci. Technol. - Rev. d'IFP Energies nouvelles* **71**, 1, 7. doi: 10.2516/ogst/2014023.

Preux C., Le Ravalec M., Enchéry G. (2016) Selecting an appropriate upscaled reservoir model based on connectivity analysis, *Oil Gas Sci. Technol. - Rev. d'IFP Energies nouvelles* **71**, 5, 60. doi: 10.2516/ogst/2016015.

Qi D., Hesketh T. (2004) Quantitative evaluation of information loss in reservoir upscaling, *Pet. Sci. Technol.* **22**, 11–12, 1625–1640. doi: 10.1081/LFT-200027875.

Rasaei M.R., Sahimi M. (2009) Upscaling of the permeability by multiscale wavelet transformations and simulation of multiphase flows in heterogeneous porous media, *Comput. Geosci.* **13**, 2, 187–214. doi: 10.1007/s10596-008-9111-0.

Renard P., de Marsily G. (1997) Calculating equivalent permeability: A review, *Adv. Water Resour.* **20**, 253–278.

Sablok R., Aziz K. (2008) Upscaling and discretization errors in reservoir simulation, *Pet. Sci. Technol.* **26**, 1161–1186. doi: 10.1080/10916460701833863.

Sanchez-vila X., Guadagnini A., Carrera J. (2006) Representative hydraulic conductivities in saturated groundwater flow, *Rev. Geophys.* **44**, 1–46. doi: 10.1029/2005RG000169.

Spiteri E.J., Juanes R. (2006) Impact of relative permeability hysteresis on the numerical simulation of WAG injection, *J. Pet. Sci. Eng.* **50**, 2, 115–139. doi: 10.1016/j.petrol.2005.09.004.

Stedinger J.R., Sule B.F., Loucks D.P. (1984) Stochastic dynamic programming models for reservoir operation optimization, *Water Resour. Res.* **20**, 11, 1499–1505. doi: 10.1029/WR020i011p01499.

Tan C.T., Homsy G.M. (1992) Viscous fingering with permeability heterogeneity, *Phys. Fluids A* **4**, 6, 1099–1101. doi: 10.1063/1.858227.

Tavakoli V. (2018) Rock typing, in: *Geological core analysis application to reservoir characterization*, pp. 85–99.

Thiele M.R., Rao S.E., Blunt M.J. (1996) Quantifying uncertainty in reservoir performance using streamtubes, *Math. Geol.* **28**, 7, 843–856. doi: 10.1007/BF02066004.

Zhang P., Pickup G.E., Stephen K.D., Ma J., Clark J.D. (2005) Multi-stage upscaling: Selection of suitable methods, *Transp. Porous Media* **58**, 191–216. doi: 10.1007/1-4020-3604-3_10.